Two-dimensional Ion-pump of Vanadium Pentoxide Nanofluidic Membrane

Raj Kumar Gogoi, Arindom Bikash Neog, Tukhar Jyoti Konch, Neelam Sarmah and Kalyan Raidongia*

Department of Chemistry, Indian Institute of Technology Guwahati, Guwahati, 781039, Assam, India.

*E-mail: k.raidongia@iitg.ac.in

1

Materials:

Hydrogen peroxide, vanadium pentoxide, potassium chloride, lithium chloride, sodium chloride and hydrochloric acid were purchased from Merck and used as received.

Preparation of flexible and freestanding membrane V_2O_5:

V_2O_5 nanosheets were prepared by treating of V_2O_5 powder with H_2O_2 in an ice cold condition.[1] Typically, 2.38 g of V_2O_5 powder was dissolved in 25 ml of deionized (DI) water placed in an ice bath followed by slow addition of 25 ml 50 % H_2O_2 under continuous stirring. Upon addition of H_2O_2 the light brown coloured solution started bubbling, and yielded a dark brown gel. The gel was then sonicated in a bath sonicator for 30 minutes and diluted with DI water. Freestanding membranes of V_2O_5 were prepared by vacuum filtration of 30 ml of 3 mg/ml aqueous dispersion of V_2O_5 nanosheets through a PTFE membrane. The as prepared membrane was allowed to dry in room atmosphere until it got detached by-itself from the PTFE membrane.

Characterization:

Nanosheets of V_2O_5 were characterized by a **Field Emission Transmission Electron Microscope (FETEM) (JEOL, Model: 2100F) and** Atomic Force Microscope (AFM) (Make: Oxford; Model: Cypher). The morphology and the cross-sections of the membranes were examined by the Field Emission Scanning Electron Microscope (Make: Zeiss, Model: Sigma). X-ray diffraction studies were carried out by employing a Bruker D-205505 Cu-Kα radiation (λ = 1.5406 Å). The hydroxyl groups present in V_2O_5 nanosheets were characterized by Fourier transform infrared (FTIR) spectrometer (Maker: PerkinElmer; Model: Spectrum Two).

Fabrication and conductivity measurements of nanofluidic devices:

Nanofluidic devices of freestanding V_2O_5 membranes were fabricated by embedding strips of the membranes of known dimensions in PDMS elastomer. The ends of the strips were exposed to electrolyte solutions by carving out reservoirs on the PDMS stub at either ends of the strip. Ag/AgCl electrodes which are connected to the terminals of a Keithley source meter (Model: 2450) were immersed in the reservoirs filled with electrolytes at both ends of the strip. The conductivity (κ) of the nanofluidic device was calculated by using the following equation:

$$\kappa = G \frac{l}{w \, x \, t} \quad .... \quad (S1)$$

Where, G = conductance, obtained from the slope of the *I-V* curve, *l*, *w* and *t* are the length, width and thickness of the strips respectively.
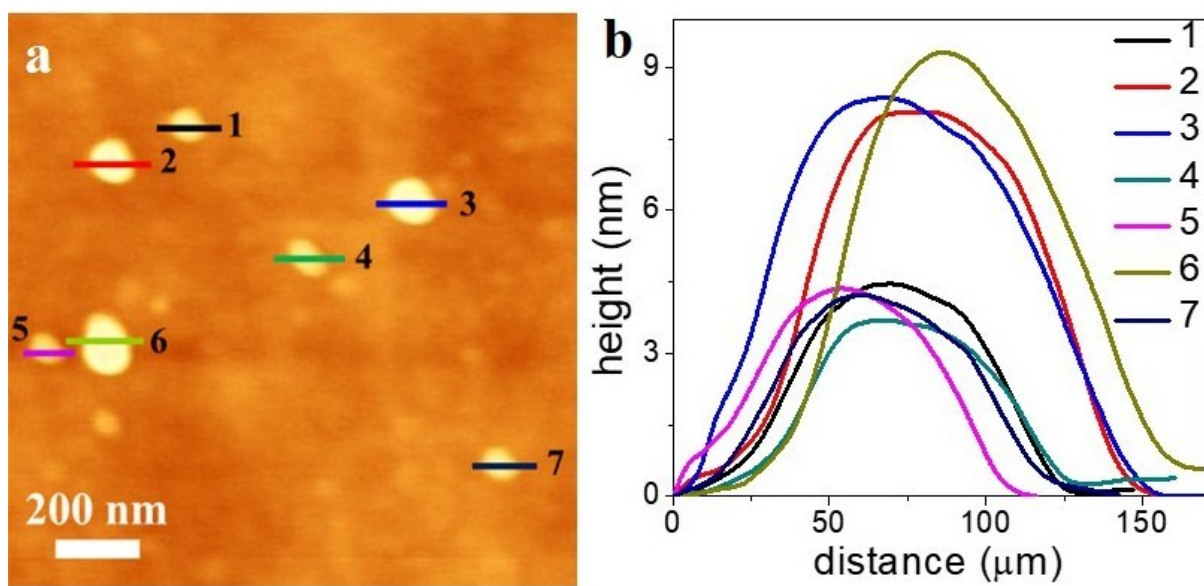
Figure S1. AFM analysis of V$_2$O$_5$ nanosheets: (a) AFM image, and (b) corresponding height profiles of V$_2$O$_5$ nanosheets.
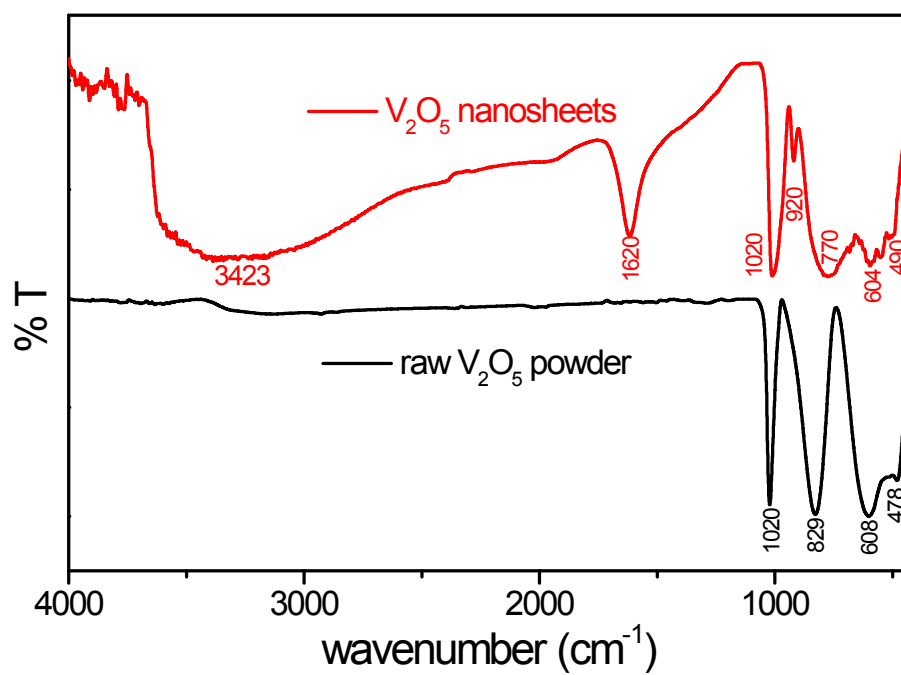
Figure S2. FTIR spectra of bulk V_2O_5 powder and exfoliated V_2O_5 nanosheets.
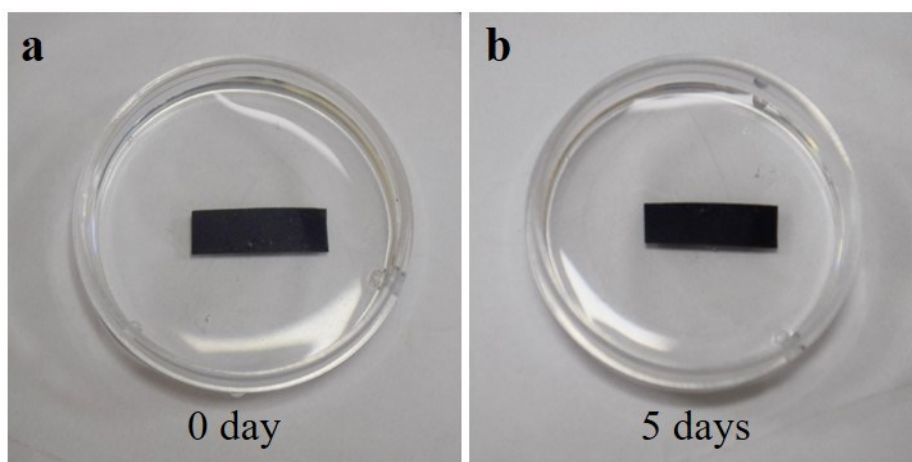
Figure S3. Stability of V$_2$O$_5$ membrane in water: Photos showing strip of a V$_2$O$_5$ membrane immerged in water at (a) 0 day and (b) after 5 days.
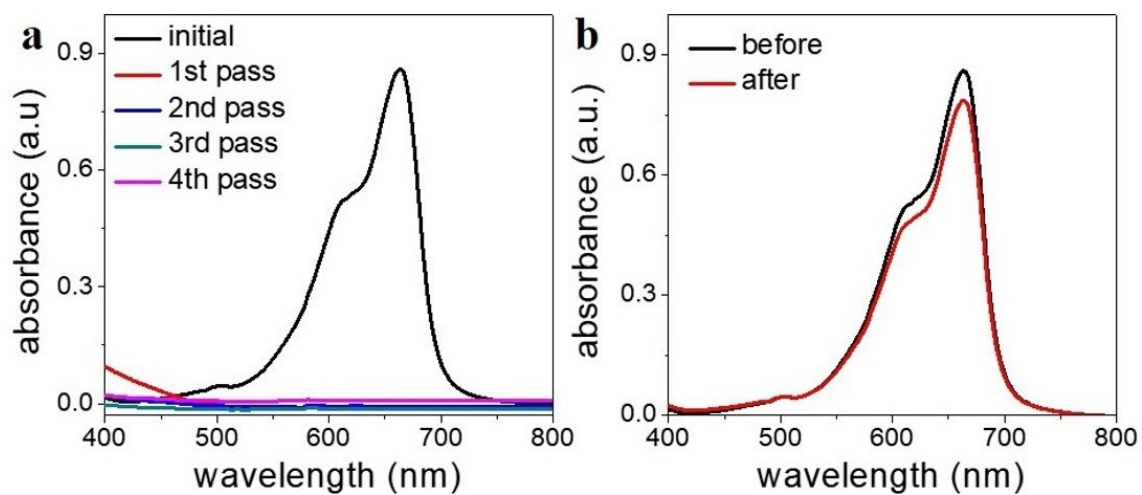
Figure S4. UV-Visible spectra comparing the absorbance of methylene blue (MB) dye before and after (a) vacuum filtration through V_2O_5 membrane, and (b) soaking of V_2O_5 membrane in aqueous dye solution.

The V_2O_5 membranes removed more methylene blue (MB) dye upon vacuum filtration than its absorption capacity, suggesting its pore sizes to be smaller than the size of dye molecules.
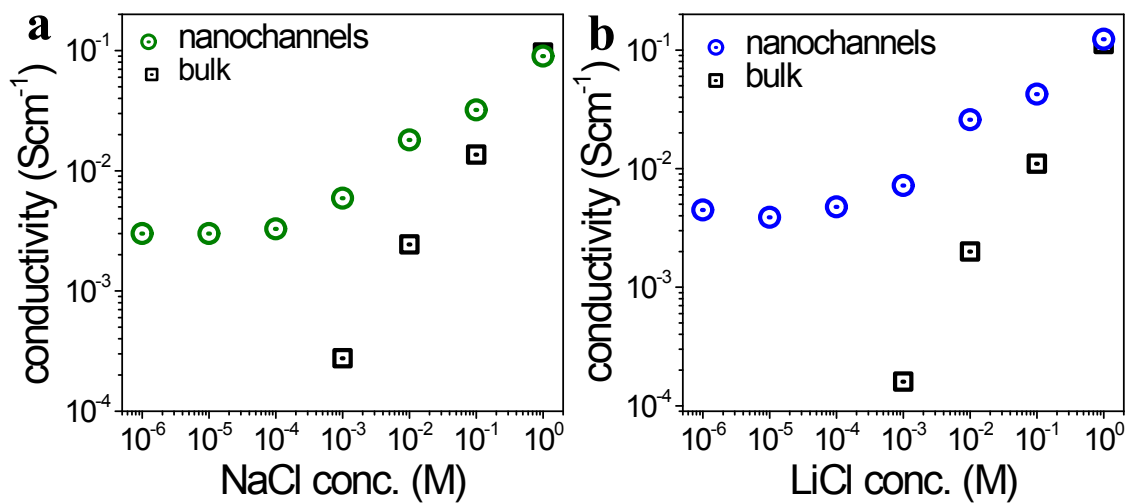
Figure S5. Ionic conductivity of V_2O_5 nanofluidic devices at different concentrations of (a) NaCl and (b) LiCl as electrolytes.
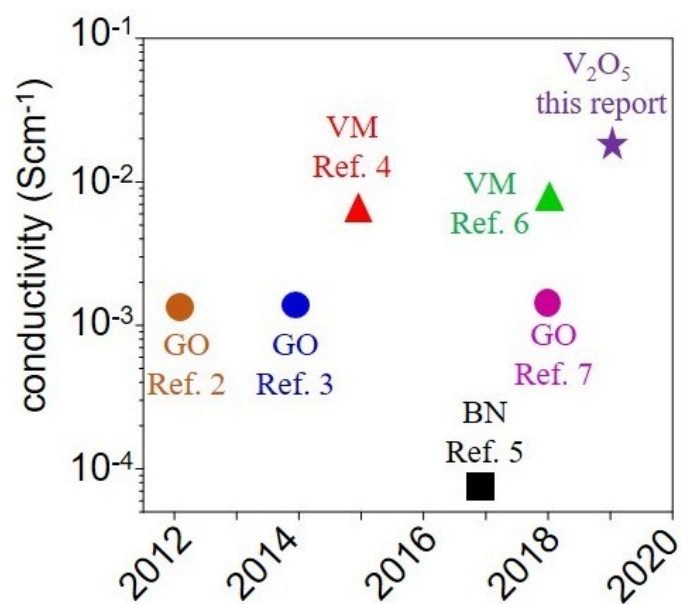
Figure S6. Comparison of proton conductivity of V_2O_5 membrane with different reconstructed lamellar membranes found in literature. (GO = graphene oxide, VM = vermiculite and BN = boron nitride.)
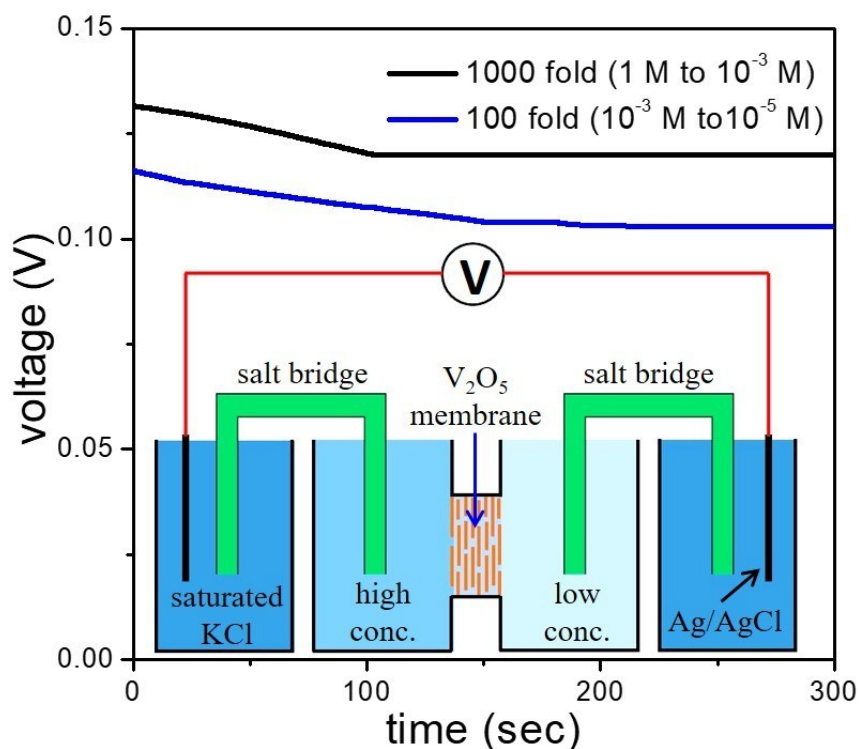
Figure S7. Ion selectivity of V$_2$O$_5$ lamellar membrane: Membrane potentials derived from concentration gradients (black line for 1000 fold concentration gradient (C$_H$ = 1M, C$_L$ = 10^{-3} M), and blue line for 100 fold concentration gradient (10^{-3} to 10^{-5} M HCl)) across the V$_2$O$_5$ membrane. Schematic illustration of the experimental set-up used for the measurement of membrane potential is shown in the inset.

The high negative zeta potential (-56 ± 1.3 mV) indicates the presence of negative charges at the surface of the V$_2$O$_5$ nanosheets, which played key roles in the selective transportation of cations through the nanochannels of the reconstructed membrane. The transference number (t_+) of cation was calculated by employing equation S2:[8,9]

$$2t_+ + 1 = \frac{E_{membrane}}{\frac{RT}{nF}ln(\frac{\gamma_H C_H}{\gamma_L C_L})} \quad \text{................... S2}$$

Where E is the membrane potential, R is gas constant, T is temperature, n is charge valent, F is Faraday constant, γ activity coefficient of ions and C_H and C_L are high and low ion

concentrations, respectively. The transference number is calculated to be 0.97, and 0.86 for low (10^{-3} to 10^{-5} M HCl), and high (1 to 10^{-3} M HCl) concentration regimes, respectively.
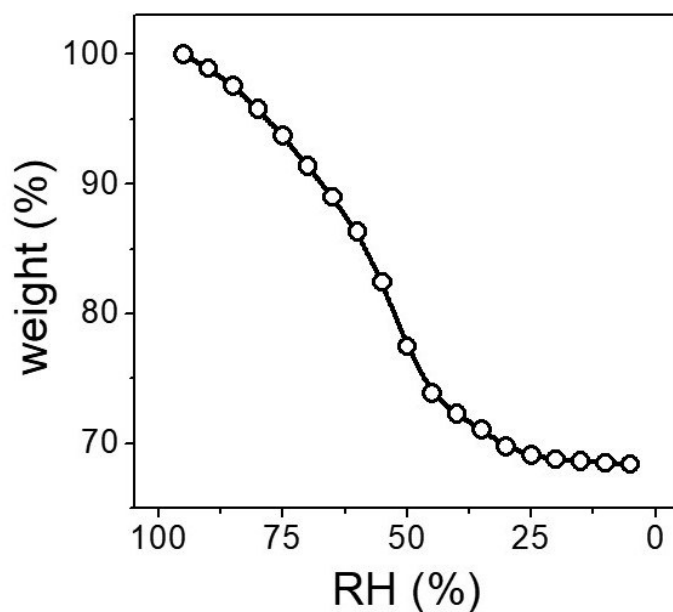
Figure S8. Weight changes of V_2O_5 membranes as a function of relative humidity (RH %).

The weight changes of V_2O_5 nanosheets membrane was measured using a digital balance, inside a closed chamber by varying the moisture content from 95 % to 5 %. The relative humidity inside the chamber was initially maintained at 95 %, which was decreased slowly by applying fused $CaCl_2$.
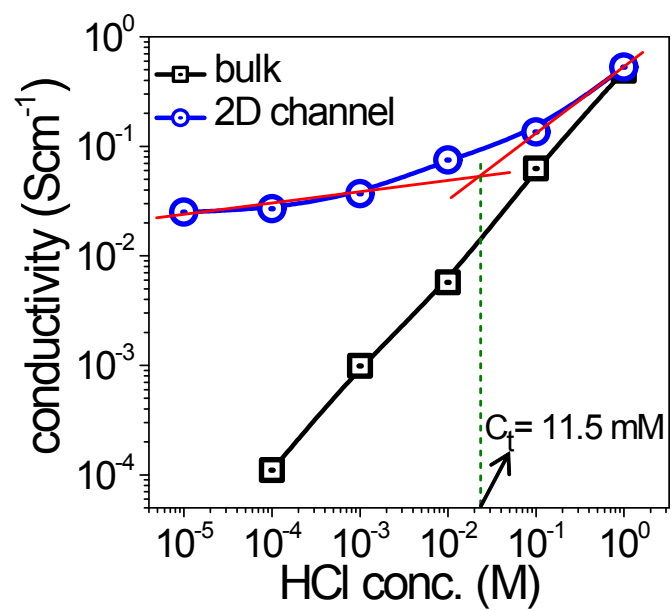
Figure S9. Determination of transition concentration (C_t) using proton conductivity curve. C_t was determined from the intersection of the lines (red) laid over the bulk and surface charge governed conductivity regimes of conductivity versus concentration plot.
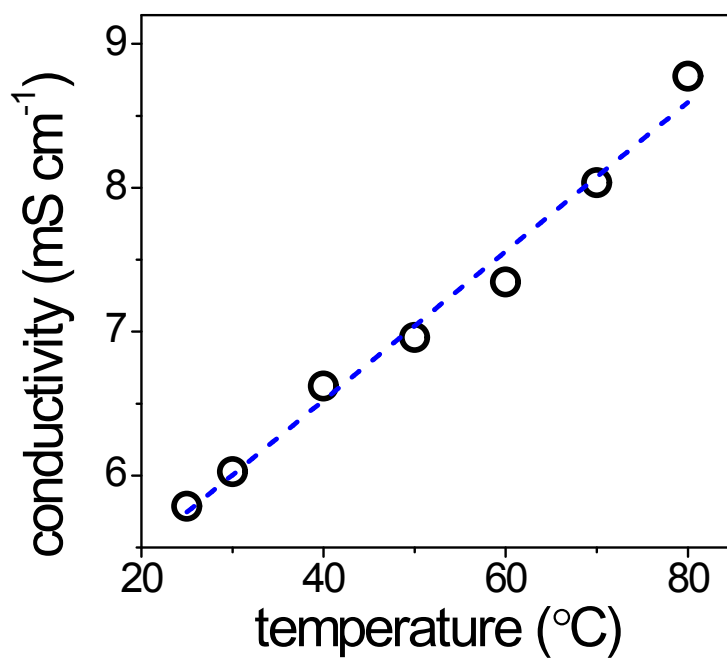
Figure S10. Proton conductivity vs temperature through V_2O_5 nanochannels with 10^{-4} M HCl.
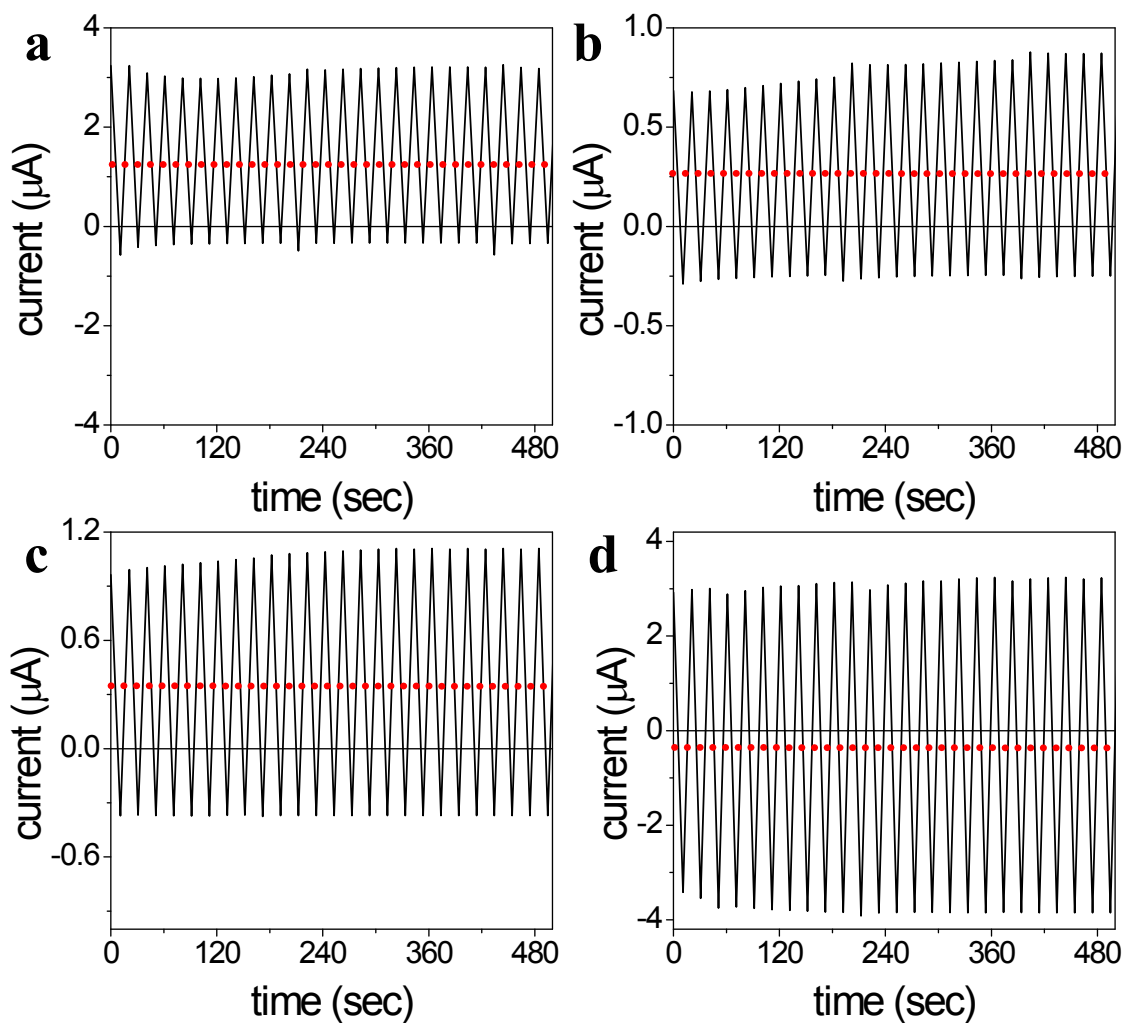
Figure S11. Plot of current as a function of time recorded under fluctuating electric field of zero mean (between +1V and -1V) through V_2O_5 triangular strip with concentration gradients of (a) 1, (b) 10, (c) 100 and (d) 10^4 folds.
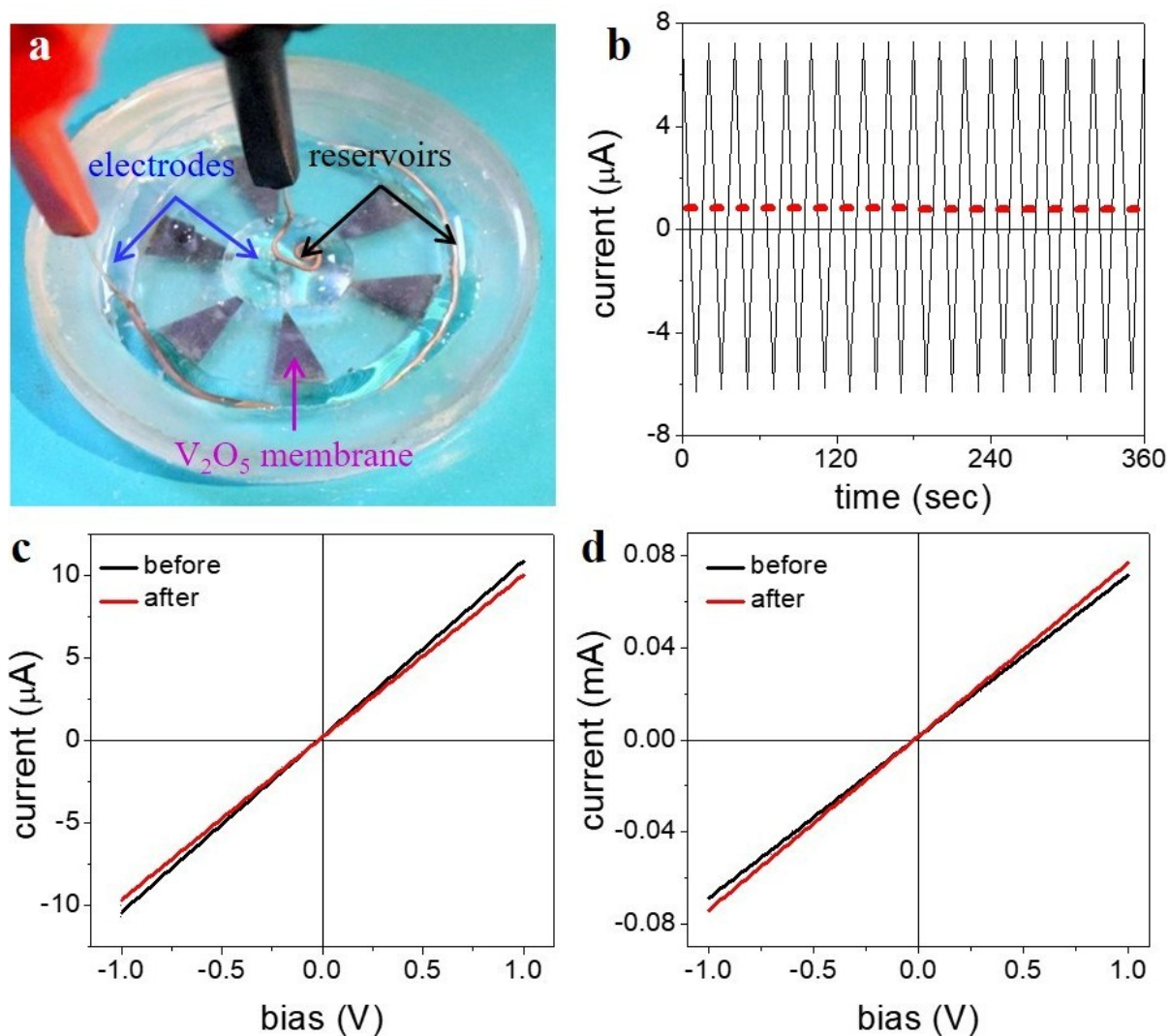
Figure S12. (a) Photo showing a V_2O_5 ion pump consisting of six triangular nanofluidic devices. (All the tips of the triangular strips are connected to same source reservoir, and similarly, all the bases are connected to the same drain reservoir). (b) Ionic current as a function of time, recorded under the fluctuating electric field of zero means (between +0.5 V and -0.5 V) through the V_2O_5 ion-pumps. The experiment was started with a 10 fold (10^{-2} (0.5 ml) to 10^{-3} M (2 ml)) concentration gradient between the reservoirs. Comparison of the *I-V* curves of the KCl electrolytes in the (c) source (low starting concentration) and (d) drain (high starting concentration) reservoirs before and after the ion pumping experiment.

The concentrations of the ions in both the reservoirs before and after the ion pumping is compared in Table S1. As evident from the table, the increase of ion concentration in the drain reservoir (high starting concentration) and that decreasing in the source reservoir (low starting concentration) confirms the ion pumping effect.

Table S1. Comparison of concentration of ions after the ion pumping in the source (2 ml 10^{-3} M KCl) and drain (0.5 ml 10^{-2} M KCl) reservoirs.

Reservoir	Initial concentration (M)	Initial conductance (S)	Final conductance (S)	Final concentration (M)	Concentration difference (M)	Avg. concentration difference (M)
Source	10^{-3}	1.1×10^{-5}	9.77×10^{-6}	8.88×10^{-4}	1.12×10^{-4}	1.12×10^{-4} $\pm$ 2×10^{-6}
	10^{-3}	1.1×10^{-5}	9.80×10^{-6}	8.90×10^{-4}	1.10×10^{-4}	
	10^{-3}	1.1×10^{-5}	9.75×10^{-6}	8.86×10^{-4}	1.14×10^{-4}	
Drain	10^{-2}	7.1×10^{-5}	7.52×10^{-5}	1.06×10^{-2}	6×10^{-4}	5.33×10^{-4} $\pm$ 5.7×10^{-5}
	10^{-2}	7.1×10^{-5}	7.49×10^{-5}	1.05×10^{-2}	5×10^{-4}	
	10^{-2}	7.1×10^{-5}	7.47×10^{-5}	1.05×10^{-2}	5×10^{-4}	

References:

1. Y. Li, C. Liu, Z. Xie, J. Yao and G. Cao, *J. Mater. Chem. A,* 2017, **5**, 16590. 2.

2. K. Raidongia and J. Huang, *J. Am. Chem. Soc.,* 2012, **134**, 16528.

3. K. Hatakeyama, M. R. Karim, C. Ogata, H. Tateishi, A. Funatsu, T. Taniguchi, M. Koinuma, S. Hayami and Y. Matsumoto, *Angew. Chem. Int. Ed.,* 2014, **53**, 6997.

4. J.-J. Shao, K. Raidongia, A. R. Koltonow and J. Huang, *Nat. Commun.,* 2015, **6**, 7602.

5. S. Qin, D. Liu, G. Wang, D. Portehault, C. J. Garvey, Y. Gogotsi, W. Lei and Y. Chen, *J. Am. Chem. Soc.,* 2017, **139**, 6314.

6. R. K. Gogoi and K. Raidongia *J. Mater. Chem. A,* 2018. **6**. 21990.

7. T. J. Konch, R . K. Gogoi, A. Gogoi, K. Saha, J. Deka, K. A. Reddy and K. Raidongia, *Mater. Chem. Front.,* 2018, **2**, 1647.

8. D. K. Kim, C. H. Duan, Y. F. Chen and A. Majumdar. *Microfluid. Nanofluid.*, 2010. **9**, 1215.

9. J. Ji, Q. Kang, Y. Zhou, Y. Feng, X. Chen, J. Yuan, W. Gua, Y. Wei and L. Jiang, *Adv. Funct. Mater.* 2017, **27**. 1603623.